Materials Science & Engineering A 618 (2014) 182–188

Contents lists available at ScienceDirect

Materials Science & Engineering A

journal homepage: www.elsevier.com/locate/msea

Microstructure, mechanical properties and fracture behavior of ultra-high strength dual-phase steel

Zhengzhi Zhao [a,b,*], Tingting Tong [a,b], Juhua Liang [a,b], Hongxiang Yin [a,b], Aimin Zhao [a,b], Di Tang [a,b]

[a] Engineering Research Institute, University of Science and Technology Beijing, Beijing 100083, China
[b] Beijing Laboratory of Modern Traffic Metal Materials and Processing Technology, Beijing 100083, China

ARTICLE INFO

Article history:
Received 27 June 2014
Received in revised form
28 August 2014
Accepted 4 September 2014
Available online 16 September 2014

Keywords:
Dual-phase steel
Annealing temperatures
Mechanical properties
Damage initiation and propagation

ABSTRACT

An ultra-high strength dual-phase steel with main components 0.16C–1.38Si–3.20Mn was produced by cold rolling followed by intercritical heat treatment. Influences of different annealing temperatures on the mechanical properties were investigated, focusing on the development of localized deformation as well as crack initiation and propagation. The work hardening behavior of tested steels after annealing was analyzed in terms of the modified C–J analysis. The experimental results indicate that the microstructures of all the tested steels contain ferrite and martensite. Annealing at 800 °C, the best comprehensive performance with a yield strength of 873 MPa, tensile strength of 1483 MPa, total elongation of 11% and yield ratio of 0.58 was achieved. Besides, the mechanisms of damage taking place in the ferrite and crack initiating at the interface between the ferrite and martensite have been observed. The crack initiating perpendicular to the lath of the martensite and then following at or near the narrowest part of a martensite ligament have also been observed. The original crack propagation exhibits a transgranular fracture feature.

1. Introduction

Development of present and future vehicles is driven by the need to simultaneously reduce mass and increase passenger and pedestrian safety. DP steel is characterized by high strength, good ductility, continuous yielding, high initial work hardening rates, and a low yield ratio of stress-to-tensile strength, which distinguishes it from other AHSS (Advanced High Strength Steel) steels [1–3].

Micro-alloying elements are usually used for different purposes in ultra-high strength steels. The effects of micro-alloying elements such as chromium (Cr), molybdenum (Mo), vanadium (V), and Niobium (Nb) on the microstructures and mechanical properties of DP steels have been intensively investigated [4–6]. However, the rise of micro-alloying elements on one hand increases the costs, and on the other hand increases the complexity of the control of process and structure. A kind of 0.16C–1.38Si–3.20Mn ultra-high strength dual-phase steel was designed in this paper without adding other alloy elements, aiming to reduce production costs, and to simplify the process.

Crack initiation and propagation in such two-phase material is not well understood and this is a limiting factor in the development and application of future generation automotive steels. Ghadbeigi et al. [7] investigated crack initiation, but they did not mention crack propagation; Saeidi et al. [8] have observed the morphology of fracture, without further study. This paper has not only observed the morphology of fracture of samples under different intercritical temperatures, but also studied the development of local deformation as well as damage initiation and propagation using in-situ tensile tests.

2. Experimental procedure

A kind of ultra-high strength dual-phase steel under different intercritical annealing temperatures, from 780 °C to 820 °C, was designed and named as samples 1–3 as given in Table 2. The chemical composition of this material and the phase transformation points Ac1, Ac3, and Ms, Mf, respectively, which were measured by DIL805 thermal dilatometer are given in Table 1. The investigated steel was prepared by a laboratory vacuum induction melting process. The gained ingot was forged into a slab which was homogenized at 1200 °C for 1 h, then was hot rolled to a thickness of 5 mm, and was finished at 850 °C. The

* Corresponding author at: Engineering Research Institute, University of Science and Technology Beijing, Beijing 100083, China. Tel.: +86 10 62332617.
E-mail address: zhaozhzhi@ustb.edu.cn (Z. Zhao).

http://dx.doi.org/10.1016/j.msea.2014.09.005
0921-5093/

Table 1
Chemical composition of the tested steel and phase transformation points.

C (wt%)	Si (wt%)	Mn (wt%)	P (wt%)	S (wt%)	Ac_1 (°C)	Ac_3 (°C)	Ms (°C)	Mf (°C)
0.16	1.38	3.20	0.008	0.004	686	849	365	259

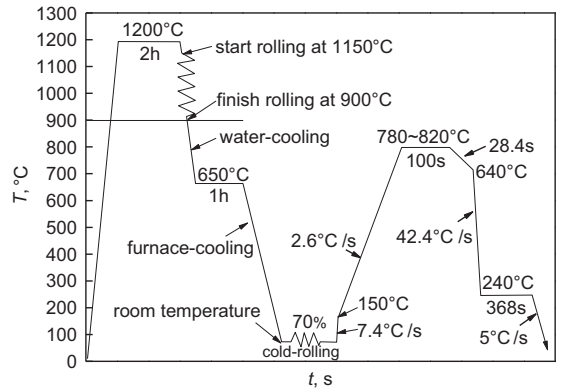

Fig. 1. Schematic diagram of the preparing process applied to tested steel.

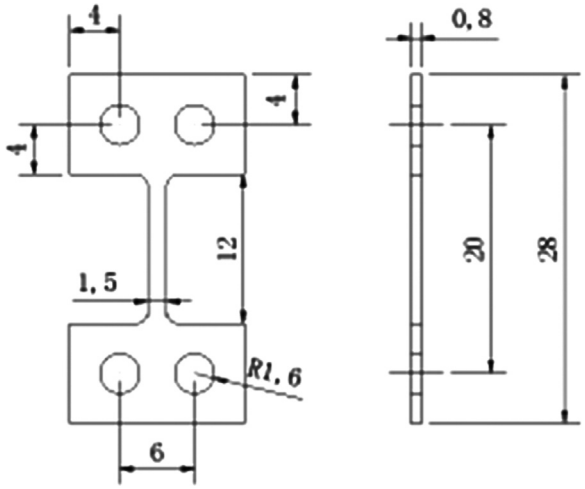

Fig. 2. In-situ tensile testing sample.

coiling was at 650 °C, followed by cooling in the furnace. Hot-rolled sheets were pickled and cold rolled to a thickness of 1.5 mm. The rectangular samples of 220 mm × 70 mm were cut from cold-rolled sheets. Continuous annealing was performed with a laboratory CCT-AY-II heat treatment system. All these steps are shown in Fig. 1.

The microstructure and fracture morphology of the tested steels were examined by scanning electronic microscopy (SEM, ZEISS ULTRA 55), transmission electron microscopy (TEM, Tecnai G2 F30 S-TWIN) and electron backscattered diffraction (EBSD, ZEISS ULTRA 55 with HKL system). Volume fraction of the martensite was estimated by the software Image-plus. Samples for SEM were mechanically polished and then were etched in a solution of 4% (volume fraction) nitric acid. Samples for EBSD measurements were electrolytically polished in a solution of 20% perchloric acid. In addition, the samples for TEM were mechanically ground to a thickness of 0.04 mm, and were electro-polished in a twin-jet machine in a solution of 5% perchloric acid and 95% alcohol at about −20 °C.

Tensile tests were carried out at 20 °C, using specimens of gage length of 50 mm, and at an initial rate of 2 mm/min. The specimen geometry shown in Fig. 2 has been used in in-situ SEM load frame to observe the damage initiation and propagation. All the samples with a dimension of 28 mm × 14 mm × 0.8 mm are cut from cold-rolled sheets with the loading direction parallel to the rolling direction. Four holes with a radius of 1.6 mm symmetrically rank on both sides of the sample. The distance between the two holes on the length direction is 20 mm. The gage length is in the middle of the sample with the length of 12 mm, width of 1.5 mm. The samples are electrolytically polished in a solution of 20% perchloric acid and are etched in a solution of 4% nitric acid.

3. Results and discussion

3.1. Microstructure of annealed steel

The microstructures of heat-treated samples are shown in Fig. 3. All the steels mainly consist of ferrite and martensite. Increasing volume fraction of the martensite is clearly observed in Fig. 3, which complies with the lever rule in the ferrite–austenite dual-phase region. According to the lever rule, increasing temperature increases the austenite volume fraction, which will transform into martensite upon quenching. And it is quite obvious that in sample 3, martensite particles are much coarser than in sample 1 and sample 2. The grain size of the martensite of steels annealed at 780 °C, 800 °C, and 820 °C were measured and they are 0.9 μm, 1.2 μm and 2.8 μm, respectively, by EBSD. This can be explained by the higher intercritical annealing temperature, which will induce the grain growth. The feature of martensites, however, is dependent on the annealing temperature. The martensite is observed with a fairly smooth surface in sample 1, whereas it appears as finely etched grains due to carbide precipitation in sample 2 and sample 3. Sample 1 is referred to as less-tempered, while sample 2 and sample 3 are referred to as well-tempered with martensite lath blurred and carbide precipitated remarkably [9], respectively. This phenomenon is caused by the tempering behavior of the martensite during aging, which is related to the alloy element contents in the austenite during intercritical region being affected by the diffusion-controlled mechanism, where the higher temperature is more effective than the lower one. This is also directly due to the enhanced tempering resistance of sample 1 because of higher alloy element contents at lower intercritical annealing temperatures [10,11].

Sample 2 was selected for a transmission electron microscope study. Fig. 4(a) shows the tempered martensite and Fig. 4(b) shows the ferrite. In Fig. 4(a), ε-carbides are visible in the martensite whose original laths have already blurred. This confirms that martensite tempering has taken place at 240 °C. In Fig. 4(b), ferrite with high-density dislocation which formed during quenching because of the squeezing by expanded martensite during transformation is clearly seen.

3.2. Mechanical properties after annealing

The mechanical properties obtained at room temperature for uniaxial tensile tests are presented in Table 2. The stress–strain diagrams for this material at different temperatures are given in Fig. 5. It can be seen that the yield strength of these steels increases with the increase of intercritical annealing temperatures. This trend is connected with the mobile dislocations in grains which have an inverse relationship with the volume fraction of softened ferrite. Furthermore, the ultimate tensile strength, which is a function of the volume fraction of the constituent phases and their hardness, decreases with the increase of intercritical annealing temperatures. As is known, increasing the volume fraction of the martensite has two contradicting effects on the tensile